Journal of Science and Technology in Civil Engineering, HUCE, 2023, 17 (2): 83–98

NUMERICAL ANALYSIS OF COMPRESSIVE BEHAVIOR OF CIRCULAR CONCRETE FILLED STEEL TUBULAR COLUMNS WITH HIGH TO ULTRA-HIGH STRENGTH MATERIALS

Hao Dinh Phan[a,*], Lien Kim Thi Dao[a]

[a]*Faculty of Civil Engineering, The University of Danang - University of Science and Technology, 54 Nguyen Luong Bang street, Lien Chieu district, Danang city, Vietnam*

Article history:
Received 21/02/2023, Revised 15/4/2023, Accepted 27/4/2023

Abstract

This paper presents a numerical analysis of the compressive behavior of short circular concrete filled steel tubular (CFST) columns having high to ultra-high strength materials under different compression loading cases. A matrix of thirty column specimens including CFST columns and empty steel tube ones was numerically investigated. Finite element models (FEMs) developed in ABAQUS were used to simulate these specimens, in which nonlinear tridimensional (3D) finite elements were chosen for modeling both inner concrete core and outer steel tube In this study, the materials of concrete and steel with compressive strength (f_c') and yield strength (f_y) ranging from 100 to 120 MPa and from 525 to 595 MPa, respectively, were used. The CFST column specimens were concentric-compressively loaded by three cases, including entirely forcing on both the steel tube and concrete core (CFE), only forcing on the concrete core (CFC), and only forcing on the steel tube (CFS). Moreover, the empty steel tubes (EST) specimens were also compressively loaded. The numerical analysis results showed that the column's mechanical behavior and load-carrying capacity mainly depend on the loading cases. In which, the CFC loading case leads to the highest load-carrying capacity and followed by the CFE loading case due to the confinement effect on the concrete core offered by the steel tube. Meanwhile, the CFS loading case results in the lowest load-carrying capacity of the CFST columns because the inner concrete core just keeps the outer steel tube more stable under compression loading compared to the EST loading case. Increasing the values of f_c' and f_y leads to a significant increase of the CFST column's load-carrying capacity in cases of CFC and CFE.

Keywords: circular concrete filled steel tubular (CFST) columns; finite element models (FEMs); high to ultra-high strength materials; different loading cases; confinement effect.

https://doi.org/10.31814/stce.huce2023-17(2)-08

1. Introduction

Recently, concrete filled steel tubular (CFST) members have been increasingly used in engineering structures such as in buildings and bridges. Because these members have an excellent combination between two constituent materials, concrete and steel, in the composite section resulting in their high load-carrying capacity (ex. compressive strength and ductility) [1]. Especially, CFST columns are widely used in highrise buildings due to their strong points (high strength and ductility, reducing the construction time) compared to the reinforced concrete (RC) columns. Therefore, choosing CFST columns is a reasonable trend to overcome some drawbacks of the RC columns such as heavy self-weight, large cross-section, low ductility, and slow construction.

CFST columns have been studied and ultilized for highrise buildings and longspan bridges in some developed countries such as United States, United Kingdom, Australia, Japan, China, etc. Hence, the mechanical behavior of CFST columns with circular and square/rectangular cross-sections were studied experimentally, analytically and numerically [1–19]. The main purposes of these previous studies

*Corresponding author. *E-mail address:* pdhao@dut.udn.vn (Phan, H. D.)

were to investigate the composite column's load-carrying capacity, the local buckling of the steel tube, the confinement effect of the concrete core and also the flexural behavior of CFST beam columns. In which, the experimental and analytical studies [1–14] were dominated, meanwhile, the numerical studies [15–19] were fewer than the other ones as mentioned above. Experimental studies have been conducted to understand the behavior of CFST columns under various loading conditions and to validate numerical models. Analytical models have been developed based on idealized assumptions, such as perfect bonding between the concrete and steel, homogeneous material properties, and uniform stress distribution. These models have provided valuable insights into the behavior of these structures, but they have limitations in predicting their behavior accurately under complex loading conditions. In recent, finite element analysis (FEA) modeling has been widely used with the support of some professional software packages. The mechanical behavior of CFST columns under different loading conditions was numerically investigated by some researchers. For axial compression loading, previous studies revealed that the cross-section shape and the width- or diameter-to-thickness ratio (B/t or D/t) of steel tube significantly affected the column's load-carrying capacity [4–7]. In which, the columns with circular sections demonstrated a better confinement effect than that with non-circular sections. Moreover, the concrete confinement effect has dramatically increased when applying axial compression on the concrete core only compared to other loading types [8, 13–15]. To model the behavior of steel tube and infilled concrete, there were different models used in previous studies [18, 19]. Most of previous studies used constituent materials with the nominal strengths ranging in the limitation that was proposed by the design standards from developed nations, for instance, AISC 360-16, EC4, and AS/NZS 2327 [20–22]. According to the three codes mentioned above, for concrete, the upper limit of compressive strength is 69, 60 or 100 MPa, respectively. Meanwile, for structural steel, the upper limit of yield strength is 525, 460 or 690 MPa, respectively. Some other studies were conducted using the constituent materials with the nominal strengths exceeding the limitation values proposed in the current design codes. To improve the beneficial characteristics of the composite section for more convenient in design of highrise building structures, the expandation of using CFST columns with high and ultra-high strength materials is necessary.

From past studies, some valuable models for both steel and concrete materials can be used to simulate the behavior of CFST columns under axially compressive loading. However, to have an accurate confined concrete model used for infilled concrete is very difficult, especially, in the case of using high and ultra-high strength materials, which have their strengths beyond the upper limit values according to AISC 360-16 [20]. In particular, to overcome the limitation of experimental database in the case of testing full-scale specimens, the research project managed by the first author has focused on performing numerical investigations on the compressive behavior of circular CFST columns with high and ultra-high strength materials. In which, the results of the numerical investigations in the case of using high to ultra-high strengh materials would be published in this research paper. The other results in the case of using high strength materials would be published in another research paper. The main purpose of this paper is to analyze the effects of some parameters such as compressive loading cases, yield strength of the steel tube, and compressive strength of the concrete core on the CFST column's load-carrying capacity, local buckling of the steel tube, and confinement effect on the concrete core.

2. Numerical modeling procedure for CFST columns

2.1. Finite element model

Building finite element models (FEMs) using the Abaqus software [23] to simulate the behavior of CFST columns under compressive loads with different loading cases is a main task in this study.

The results of the numerical analysis of stress and strain distribution in the column will give a better understanding of the mechanical behavior of this composite structure type. The requirement is that the FEMs should be built so that the simulation results accurately reflect the real-life behavior of the composite column, including the mechanical properties of the constituent materials, the interaction between the steel tube and concrete core, the connection details, etc. The simulation is performed for the various components that make up the CFST column, including steel tube, concrete core, and loading plates.

The steel tube, concrete core, and loading plates are components that interact with each other during loading process. To accurately simulate the actual behavior of CFST columns, these components need to be modeled using appropriate elements. In which, the Solid 8 node (C3D8) element is used to simulate the steel tube, loading plates, and the concrete core for layers located outside the center axis of the column. Meanwhile, the Solid 6 node (C3D6) element is used for the concrete core near the center axis of the column. The finite element types used to simulate the mentioned components above are shown as in Fig. 1. To have more accurate analysis results, the mesh size convergence was carried out to select reasonable meshes for steel tube and concrete core components. For instance, a typical meshing of steel tube (30×30 mm) and concrete core (50×50 mm) is presented as shown in Fig. 2. The interaction surfaces between the steel tube and the concrete core, as well as between the steel tube, concrete core and the loading plates, are modeled using corresponding interaction and bonding models availabe in Abaqus software.

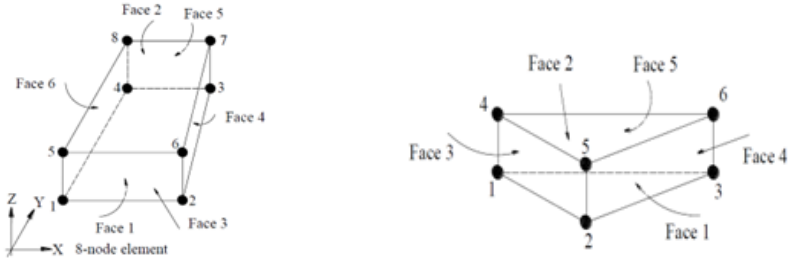

(a) The solid element with eight nodes (b) The solid element with six nodes

Figure 1. Types of finite elements

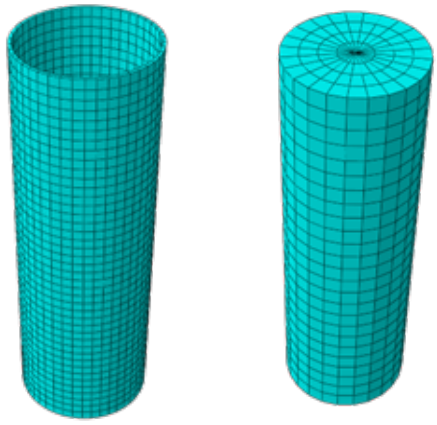

Figure 2. Meshing for steel tube and concrete core

2.2. *Constituent material models*

To have rational and accurate concrete model for discribing behavior of the concrete material in a CFST column, especially in the case of large-scale specimens, is allways very challenging for the simulation process. In previous studies, there were some concrete models that can be available for modeling the CFST columns under axial compression [24–28]. However, each model has its own limitation in accurately modeling the compressive behavior of these composite structures. Hence, a concrete damaged plasticity (CDP) material model available in ABAQUS needs to be developed with consideration of the confinement effect for use in the modeling process in this paper. A new confined concrete model has been developed by the first author based on the literature from previous concrete models. The proposed confined concrete model used to discribe the compressive behavior of the concrete core filled in the steel tube of circular CFST columns in this study was shown as in Fig. 3. The accuracy and confidence of this confined concrete model would be validated in Subsection 2.5.

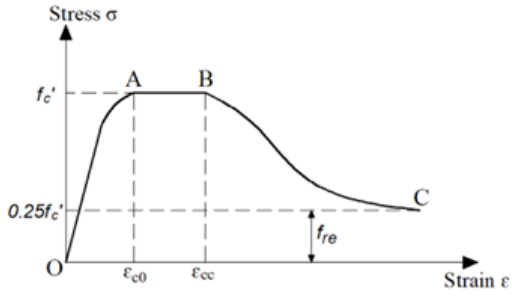

Figure 3. A proposed confined concrete model

There are three main stages for the compressive behavior of confined concrete material that was filled in the circular steel tube including the ascending stage OA, the plateau stage AB, and the descending stage BC as can be seen in Fig. 3. Herein, the first stage (OA) was constructed based on the confining concrete material law suggested by Samani and Attart [27] using the relationship as in Eq. (1).

$$\frac{\sigma_{(OA)}}{f_c'} = \frac{A \times \left(\frac{\varepsilon}{\varepsilon_{c0}}\right) + B \times \left(\frac{\varepsilon}{\varepsilon_{c0}}\right)^2}{1 + (A-2) \times \left(\frac{\varepsilon}{\varepsilon_{c0}}\right) + (B+1) \times \left(\frac{\varepsilon}{\varepsilon_{c0}}\right)^2} \qquad 0 < \varepsilon \leq \varepsilon_{c0} \tag{1}$$

where

$$A = \frac{E_c \times \varepsilon_{c0}}{f_c'}; \quad B = \frac{(A-1)^2}{0.55} - 1$$

The strain at the peak stress of the unconfined concrete ε_{c0} (point A) was proposed by Tasdemir et al. [24] based on the regression analysis of previous test specimens' database. The relationship between ε_{c0} and f_c' is expressed as in Eq. (2).

$$\varepsilon_{c0} = \left(-0.067 \times (f_c')^2 + 29.9 \times f_c' + 1053\right) \times 10^{-6} \tag{2}$$

The second stage (AB) with the peak stress value remains constant in a range of strain from ε_{c0} to ε_{cc}. This stage illustrates the increase of strain at the same value of peak stress. It means that the ductility of concrete develops due to the confinent effect on the concrete core offered by the steel tube. In which, the confined strain ε_{cc} at the point B can be determined as in Eq. (3) that was proposed by Xiao et al. [26].

$$\frac{\varepsilon_{cc}}{\varepsilon_{c0}} = 1 + 17.4 \times \left(\frac{f_r}{f_c'}\right)^{1.06} \tag{3}$$

where f_r represents a confining stress, it depends on some related values such as f_c', f_y and D/t. The value of f_r can be calculated based on regression analysis as shown in Eq. (4).

$$f_r = \left[\frac{1 + 0.03224 \times f_y}{1 + 1.52 \times 10^{-6} (f_c')^{-4.5}}\right] \times \exp\left(-0.0212 \times \frac{D}{t}\right) \tag{4}$$

The third stage (BC) is an exponential function proposed by Binici [25], it describes the decline of compressive strength of concrete from f_c' to f_{re}. In which, the relationship between stress and strain in this stage is presented as in Eq. (5).

$$\sigma_{(BC)} = f_{re} + (f_c' - f_{re}) \times \exp\left[-\left(\frac{\varepsilon - \varepsilon_{cc}}{\alpha}\right)^{\beta}\right] \varepsilon \geq \varepsilon_{cc} \tag{5}$$

Three key parameters in Eq. (5) including the residual stress the cofficients and are proposed by Tao et al. [28], as can be seen in Eqs. (6) and (7).

$$f_{re} = 0.7 \times \left(1 - e^{-1.38\xi_c}\right) \times f_c' \leq 0.25 \times f_c' \tag{6}$$

$$\alpha = 0.04 - \frac{0.036}{1 + e^{6.08\xi_c - 3.49}}; \quad \beta = 1.2 \tag{7}$$

In the Eqs. (6) and (7), $\xi_c = A_s f_s / A_c f_c'$, is the confinement factor in a CFST column. In which , is the cross-section area of the steel tube and concrete core, respectively.

In this paper, the high to ultra-high strength concrete with compressive strength ranging from 100 to 120 MPa was used. The elastic modulus was calculated based on the formula proposed in ACI 318-19 [29]. The main mechanical properties of concrete material are illustrated as in Table 1.

Table 1. Mechanical properties of concrete material

Mass density (kg/m^3)	Compressive strength, f_c' (MPa)	Elastic modulus, E_s (MPa)
2400	100	47000
	110	49294
	120	51486

For modeling material properties of the steel tube component in ABAQUS, the elasto-plastic model as shown in Fig. 4, is reasonable to use in this study. In the elastic stage, linear stress-strain behavior is defined based on the yield strength (f_y) and modulus of elasticity (E_s) of steel material. In which, f_y is chosen as the nominal steel strength, and E_s is taken as 200 GPa with Poisson's ratio (ν_s) of 0.3 in modeling process The steel tubes used herein have the yield strength with three levels including 525, 560, and 595 MPa.

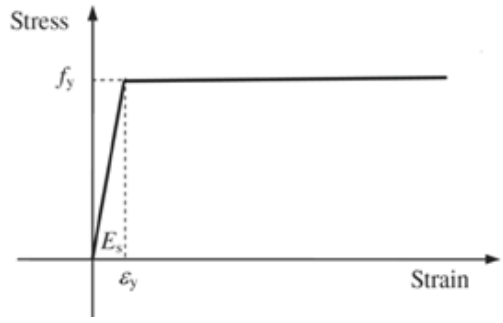

Figure 4. Elasto-plastic model for the steel tube

2.3. Steel-concrete interaction model

For steel-concrete interaction discribing in the case of CFST columns under axial compressive loading condition, the *Contact pair option with surface-to-surface contact type was used to model the interaction between the inner surface of steel tube and the outer surface of concrete core. A pair

of surfaces in this contact including master and slave surfaces requires to be defined. To reduce numerical errors, the slave surface should belong to a softer component, the steel tube, and has a finer mesh than the master one, the concrete core [23]. The contact property between the master and slave surfaces was defined by normal behavior and tangential behavior. In which, the normal behavior is simulated by the "Hard" contact which allows for the separation of the two surfaces after contact. The tangential behavior between the two surfaces is simulated by the Coulomb friction model with a friction coefficient taken as 0.2 [15].

2.4. Boundary conditions and loading applying

There are three loading cases for CFST columns including entirely forcing on both the steel tube and concrete core (CFE), only forcing on the concrete core (CFC), and only forcing on the steel tube (CFS). Besides, the empty steel tubes (EST) specimens were also compressively loaded in this study. The dimensions of the composite and steel column specimens, and the different loading cases are shown as in Fig. 5. Hence, the boundary conditions and loading application would be setup so that it accurately reflects the real-life behavior of these columns.

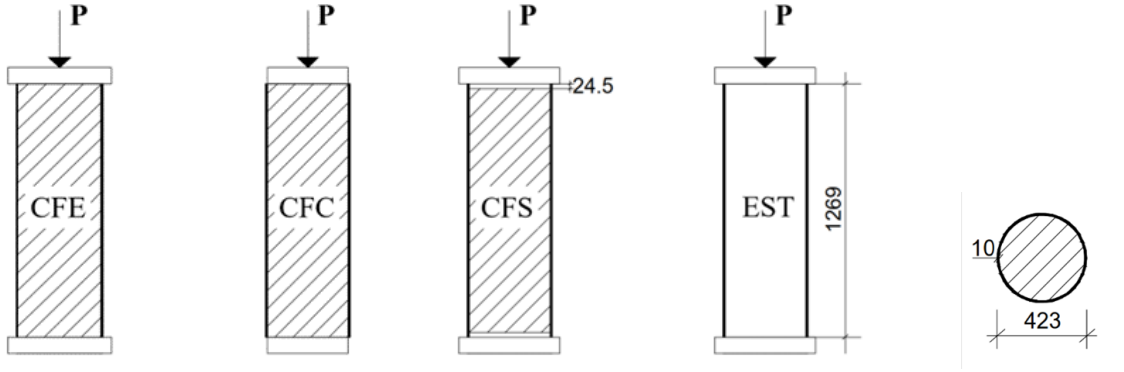

(a) Load applied to the entire section (b) Load applied to the concrete section (c) Load applied to the steel section (d) Load applied to the empty steel tube section (e) The section of the CFST columns

Figure 5. Dimensions of the column and different loading cases

According to the loading case, the loading plates with a rigid material or an assumption material similar to the rigid material would be selected. In this paper, the asumption material having elastic modulus $E = 10^9$ and Poisson coefficient $\nu = 10^{-6}$ (nearly rigid material) was chosen for material properties of the loading plates in the CFE, CFS and EST loading cases. The Reference Point (RP) function in ABAQUS was used to set up boundary conditions and apply axial compression loads directly on the concrete core surface for the CFC loading case. Meanwhile, boundary conditions and compressive load were applied at two ends of the column through the RPs connected to th surfaces of loading plates the three remaining cases. In which, the column was fully fixed at the bottom end through the first RP with all six degree of freedom (DOF) being prevented and partially fixed at the top end through the second RP with five DOF being prevented and one DOF being released so that this end can move along the longitudinal axis of the column. In the cases of using loading plates the contact between concrete core surfaces as well as steel tube surfaces at two column's ends and the loading plates would be 'Tie' connection proposed in ABAQUS library.

The displacement method for applying axial conpressive loads on the column specimens was selected in this study. In which, the increase of the axial displacement step by step from zero value was applied at the RP loacated on the center of the loading plate (for CFE, CFS and EST loading

cases) or on the center of the concrete cross-section (for CFC loading case) of the column's top end. The RPs were used to ensure that all points located on the top surface of the loading plate or the concrete core have the same displacement in the loading process. It means that the axial compressive load is evently distributed on the column's top end during the loading process. The RPs for applying axial compressive loads were chosen at the points putting the concentrated force P as can be seen in Fig. 5. In this paper, the reasonable value of upper margine for the displacement loading range is 20 mm selected for all column specimens

2.5. Modeling validation

The FEMs developed using the confined concrete model for concrete core and elasto-plastic model for the steel tube proposed in this study were validated by both the experimental and numerical results collected in previous studies [8, 15] with a good agreement. The details of the compressive strength (compressive load-carrying capacity) comparison between proposed models and previous studies are shown in Table 2. The validated FEMs then were used to conduct parametric studies to investigate the effects of some parameters including loading case, compressive strength of concrete f_c' and yield strength of steel f_y as mentioned above on the compressive strength and also deformation capacity of circular CFST columns. The numerical simulation results and discussions would be presented in detail in the next section.

Table 2. Compressive strength comparison between proposed models and previous studies

Loading case	P_{Exp} (kN)	P_{Num} (kN)	$P_{\max}$ (kN)	$P_{\max}/P_{Exp}$	$P_{\max}/P_{Num}$
CFE	2150	2334	2321	1.08	0.99
CFC	2220	2914	2763	1.24	0.95
CFS	950	994	994	1.05	1.00
EST	920	1008	987	1.07	0.98

Notes: P_{Exp} is the axial compressive load-carrying capacity of the column with different loading cases from the experimental results conducted by Johansson and Gylltoft [8]; P_{Num} is the axial compressive load-carrying capacity of the column with different loading cases from the numerical simulation results conducted by Phan and Trinh [15]; $P_{\max}$ is the axial compressive load-carrying capacity of the column with different loading cases from the numerical simulation results in this paper.

3. Parametric studies, results and discussions

3.1. Loading cases and nominal compressive strengths of CFST columns

The large-scale circular CFST columns subjected to axial compressive loads with different loading cases were simulated using Abaqus software. Herein, geometric features of the CFST column including the outer diamester of steel tube D = 423 mm, the thickness of steel tube t = 10 mm, and the column's heigth H = 1269 mm ($3D$) were chosen as can be seen in Fig. 5.

In this study, the column specimens were subjected to concentrically compressive loads with purpose to analyze, estimate the mechanical behavior of the CFST columns As mentioned in Subsection 2.4, there are three loading cases for CFST columns, namely CFE, CFC and CFS, and one loading case for empty steel tubes, EST. All loading cases for circular CFST columns and empty steel tubes were simulated under the compressive loading with the change at three levels for two other parameters including the compressive strength of concrete material (100, 110, and 120 MPa) and the yield strength of steel material (525, 560, and 595 MPa). The matrix of the composite columns and steel tubes used for the simulation process were shown as in Table 4.

To compare with the numerical results, the nominal strength of CFST columns in this paper need to be predicted based on a design code. As discussion in the literature related to three design codes including AISC 360-16, EC4, and AS/NZS 2327 [20–22], the upper strength limits of concrete and steel materials used in these standards are almost less than the strength ranges of materials used in this study. In which, the EC4 has the lowest values for upper strength limitations, then the AISC 360-16 stands in the middle, and the AS/NZS 2327 has the highest values for upper strength limitations. Hence, to have refereed values for numerical simulation results, the authors selected the AISC 360-16 with the middle values of upper strength limits to determine the nominal compressive strength of circular CFST columns as below. It would help to estimate how difference of the load-carrying capacity of the composite column using high strength materials between the AISC 360-16 preditions and the FEM simulation results. This comparison leads to widern the related knowledge in the range of high strength materials, and then have more detailed studies for developing the application of AISC 360-16 in designing composite structures in the future.

Assuming that there is a full interaction between the steel tube and the concrete core, the nominal compressive strength P_0 of a circular CFST column was calculated according to the American design code AISC 360-16 [20] as shown in Eq. (8). The results of the nominal compressive strength of CFST columns using steel and concrete materials with different yield strength and compressive strength levels were presented as in Table 3.

$$P_0 = A_s f_s + 0.95 A_c f_c' \tag{8}$$

where, A_s, A_c is the cross-section area of the steel tube and concrete core, respectively; f_s, f_c' is the yield strength of steel material and the compressive strength of concrete material, respectively. In which, $P_s = A_s f_s$, is the compressive strength contribution by the steel tube component, and $P_c = 0.95 A_c f_c'$, is the compressive strength contribution by the concrete core component.

Table 3. Compressive strength of circular CFST columns according to AISC 360-16

D (mm)	t (mm)	A_s (mm^2)	f_s (MPa)	A_c (mm^2)	f_c' (MPa)	P_0 (kN)	P_s (kN)	P_c (kN)
423	10	12975	525	127491	100	18923	6812	12112
423	10	12975	525	127491	110	20135	6812	13323
423	10	12975	525	127491	120	21346	6812	14534
423	10	12975	560	127491	100	19378	7266	12112
423	10	12975	560	127491	110	20589	7266	13323
423	10	12975	560	127491	120	21800	7266	14534
423	10	12975	595	127491	100	19832	7720	12112
423	10	12975	595	127491	110	21043	7720	13323
423	10	12975	595	127491	120	22254	7720	14534

3.2. FEM results of columns' compressive strengths

The numerical results including compressive strengths or load-carrying capacities, and axial force vs displacement relationships of all specimens are shown in Table 4, and Figs. 6–8, respectively. Meanwhile, several typical failure modes and axial force distribution in concrete core and steel tube components of some column specimens are also illustrated in Figs. 9–11 and Fig. 12, respectively. The detailed results and discussions would be presented herein and in next sub-sections.

Compressive strengths or load-carrying capacities of all thirty column specimens from the numerical results by FEM in this study, symbol as P_{max}, and the calculated results by AISC 360-16, symbol

as P_0, are presented as in Table 4. In which, the results from FEM corresponding with different loading cases were compared to the results predicted by the American design code AISC 360-16.

Table 4. Compressive strength comparison between FEM (P_{max}) and AISC 360 (P_0 or P_s)

Specimen	Load case	f_y (MPa)	f'_c (MPa)	P_{max} (kN)	P_0 (kN)	P_s (kN)	$P_{max}/P_0(P_s)^*$
C-CFE-525-100	CFE	525	100	22909	18923	6812	1.21
C-CFE-525-110			110	24044	20135	6812	1.19
C-CFE-525-120			120	25813	21346	6812	1.21
C-CFE-560-100		560	100	23190	19378	7266	1.20
C-CFE-560-110			110	24660	20589	7266	1.20
C-CFE-560-120			120	26388	21800	7266	1.21
C-CFE-595-100		595	100	23232	19832	7720	1.17
C-CFE-595-110			110	24640	21043	7720	1.17
C-CFE-595-120			120	26126	22254	7720	1.17
C-CFC-525-100	CFC	525	100	26391	18923	6812	1.39
C-CFC-525-110			110	27709	20135	6812	1.38
C-CFC-525-120			120	29432	21346	6812	1.38
C-CFC-560-100		560	100	27215	19378	7266	1.40
C-CFC-560-110			110	28507	20589	7266	1.38
C-CFC-560-120			120	29956	21800	7266	1.37
C-CFC-595-100		595	100	27971	19832	7720	1.41
C-CFC-595-110			110	29315	21043	7720	1.39
C-CFC-595-120			120	30623	22254	7720	1.38
C-CFS-525-100	CFS	525	100	65834	18923	6812	0.97
C-CFS-525-110			110	65834	20135	6812	0.97
C-CFS-525-120			120	65834	21346	6812	0.97
C-CFS-560-100		560	100	6966	19378	7266	0.96
C-CFS-560-110			110	6966	20589	7266	0.96
C-CFS-560-120			120	6966	21800	7266	0.96
C-CFS-595-100		595	100	7353	19832	7720	0.95
C-CFS-595-110			110	7353	21043	7720	0.95
C-CFS-595-120			120	7353	22254	7720	0.95
C-EST-525	EST	525		6511		6812	0.96
C-EST-560		560		6871		7266	0.95
C-EST-595		595		7279		7720	0.94

*Notes: P_{max} is compared to P_0 in the CFE and CFC loading cases; and P_{max} is compared to P_s in the CFS and EST loading cases.

From the comparison results in Table 4, it can be seen that the compressive strength or load-carrying capacity of the CFST column in the CFC loading case reaches the highest value at different levels of f_y and f'_c. Namely, the increase in the compressive strength of the corresponding CFST columns obtained from FEM compared to that of CFST columns calculated according to AISC 360-16

is about 37-41%. The outstanding compressive strength of CFST columns in this loading case revealed that when applying axial compressive load onto the concrete core leading to perfect confinement action. Next is the CFE loading case, which increases the compressive strength of the CFST column by about 17-21% with the same comparing reference. This result demonstrated that when applying axial compressive load onto the whole composite section of the CFST column the concrete core is confined by steel tube but with lower effect compared to the previous loading case. Meanwhile, the two remaining loading cases, CFS and EST, show that mainly only the steel tube participates in compression force, while the concrete core only prevents local buckling of the steel tube inward. The comparison data shows the compressive strength of the columns in the CFS and EST loading cases, $P_{\max}$ (FEM), reaches about 95-97% and 94-96%, respectively, compared to the compressive strength of the steel tube component in the CFST column, P_s (AISC 360-16).

3.3. Axial force – displacement relationships

The diagrams depicting the relationship between the compressive force and axial displacement ($P - \Delta$) of CFST columns and corresponding hollow steel columns using steel and concrete materials with different yield strengths and compressive strengths under different loading cases mentioned above are shown as in Figs. 6–8. In general, the force vs displacement curves of CFST columns with different loading cases obtained from the numerial modeling are reasonable. In which, the CFST columns in CFE and CFC loading cases have better mechanical behavior with high compressive stiffness and load-carrying capacity compared to the CFST columns in CFS loading case and for the empty steel tubes under the compressive loading. It is due to the confined effect on the concrete core offered by the steel tube and the slowerbuckling or none-buckling of the steel tube during the comprssive process for the CFE and CFC loading cases, respectively. The detailed analysis related to mechanical behavior of these columns would be performed as below.

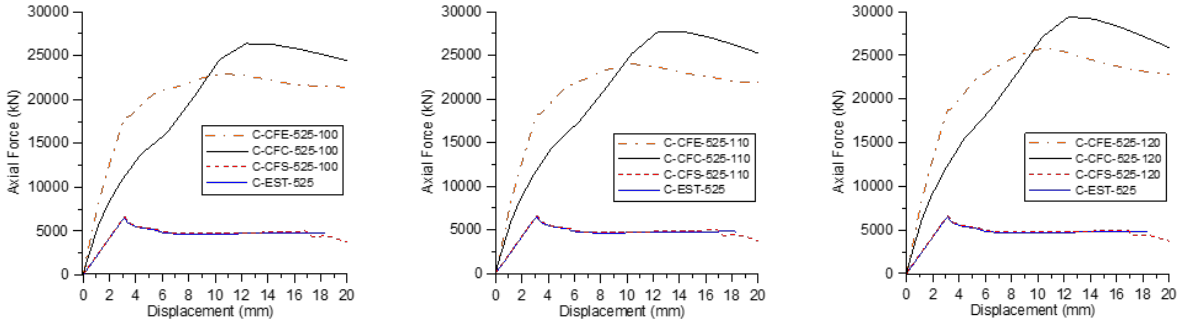

(a) f'_c = 100 MPa (b) f'_c = 110 MPa (c) f'_c = 120 MPa

Figure 6. Axial force – displacement relationship (f_y = 525 MPa)

The $P - \Delta$ curves in Figs. 6–8 show that among all the levels of f_y and f'_c of the constituent materials, in the elastic stage, the CFE loading case results in the stiffest compressive behavior of the composite column, followed by the CFC loading case, and lastly the remaining two loading cases, CFS and EST. The difference of compressive stiffness of CFST column between CFE and CFC loading cases depends on the load transfering onto the steel tube and concrete core components. In the elastic stage, for the first case CFE, both steel tube and concrete core bear the axial load so the compressive stiffness of the composite column coming from two constituent components simutaneously. Meanwhile, for the second case CFC, the concrete core bears the axial load directly and step by step the steel tube would receive the load transfered by the concrete core later so the compressive stiffness of the composite column mainly coming from the concrete core in this stage Conversely, in the

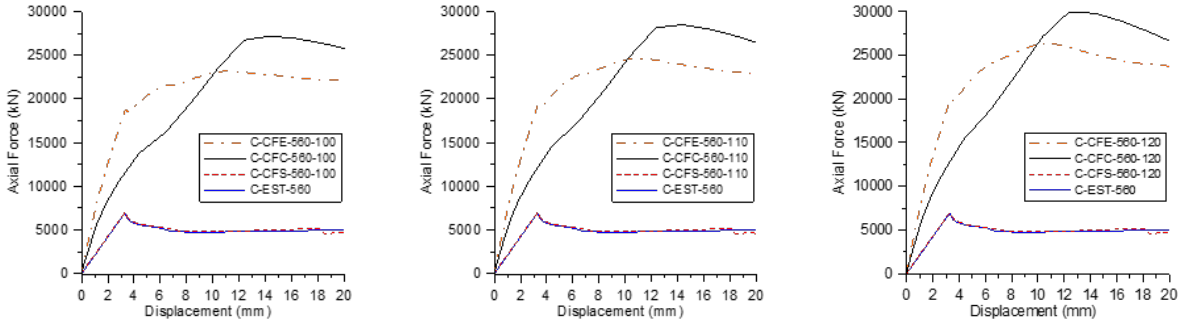

(a) f_c' = 100 MPa (b) f_c' = 110 MPa (c) f_c' = 120 MPa

Figure 7. Axial force – displacement relationship (f_y = 560 MPa)

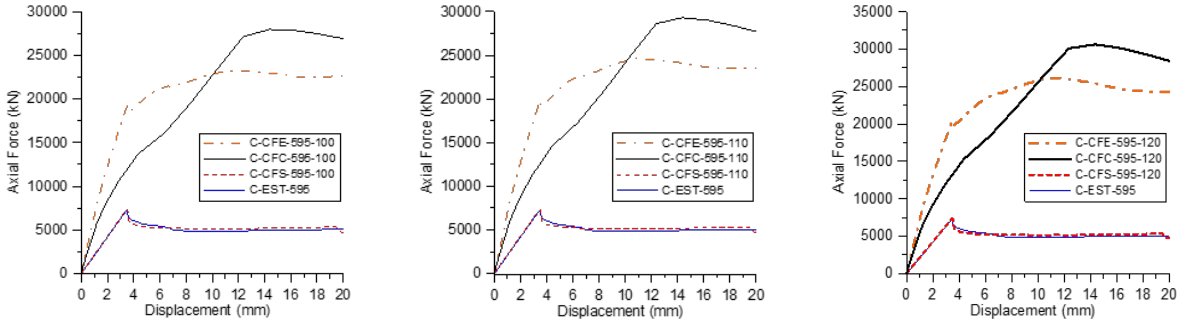

(a) f_c' = 100 MPa (b) f_c' = 110 MPa (c) f_c' = 120 MPa

Figure 8. Axial force – displacement relationship (f_y = 595 MPa)

post-elasticity and strength recovery stage, the stiffness of the composite column in the CFC loading case is larger than in the CFE loading case. This behavior has demonstrated that for the later stage of compressive loading the deformation of the composite column with two constituent materials having different mechanical properties results in the change of compressive stiffness. In which, for the CFE loading case, the higher Poisson coefficient of steel compared to that of concrete material and the negligible effect of bond strength between steel tube and concrete core surfaces might reduce the confinement effect offered by the steel tube onto the concrete core so the compressive stiffness of the CFST column has a reduced trend. Moreover, the outward buckling of the steel tube occurring in this loading case may result in the lower compressive stiffness. Meanwhile, for the CFC loading case, the deformation of the concrete core combined with non-buckling of the steel tube and the significant bond strength development lead to the increase of the confinement effect, so the CFST column has higher compressive stiffness and load-carrying capacity. It demonstrates reasonable behavior in this stage of the CFST column with different loading cases [8]. The remaining two loading cases CFS and EST have no strength recovery stage, but after reaching the peak value, the compressive strength decreases suddenly due to local buckling of the steel tube wall. The results revealed that in the case of loading on the steel tube of the CFST column (CFS), the concrete core does not bear axial compressive load, it just prevents the local buckling inward of the steel tube wall only. This is a small benefit effect compared to that coming from the EST loading case.

3.4. Failure modes of column specimens

The failure modes of the column specimens corresponding to four loading cases when using the constituent material combinations with $f_y = 525, f_c' = 100$ (MPa); $f_y = 560, f_c' = 110$ (MPa); and $f_y = 595, f_c' = 120$ (MPa) are shown in Figs. 9–11. The comparison and failure analysis of the column specimens helps to expand the understanding of the mechanical behavior of CFST columns as well as empty steel tube columns when using high to ultra-high strength materials in different compression loading cases.

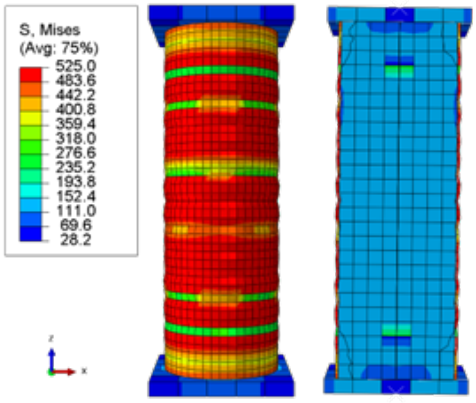

(a) C-CFE-525-100

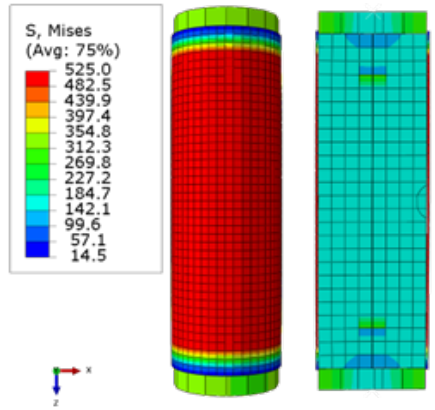

(b) C-CFC-525-100

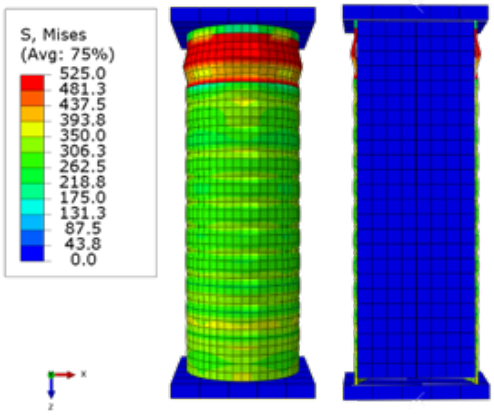

(c) C-CFS-525-100

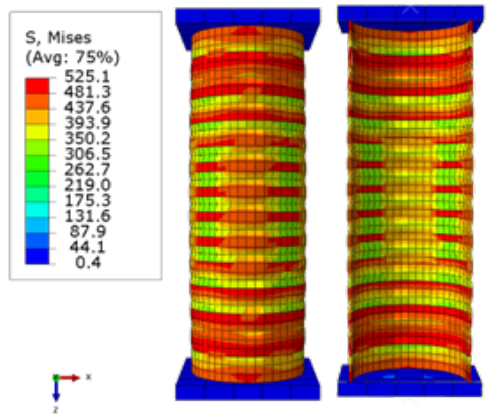

(d) C-EST-525

Figure 9. Failure modes of the columns with $f_y = 525, f_c' = 100$ (MPa)

Based on the image of deformation and stress distribution on the steel tube and concrete core, it is found that the different compressive loading cases significantly affect the failure mode of the component members as well as the overall column. For the two loading cases CFE and CFC, the deformation and stress distribution on the steel tube and concrete core are approximately symmetrical across the cross-section in the center of the column. However, there is a difference in the CFE loading case of failure due to the steel tube reaching yield strength f_y and slight local buckling along with cracking of the core concrete, and the CFC loading case failure due to steel tube reach yield strength f_y with cracking of core concrete. Furthermore, the compressive stress in the concrete core of the CFC loading case is higher than that of the CFE loading case when considering the same material grade of steel tube and concrete core components (Figs. 9–11(a), (b)).

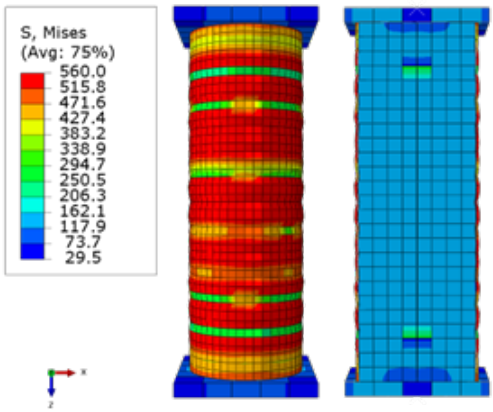

(a) C-CFE-560-110

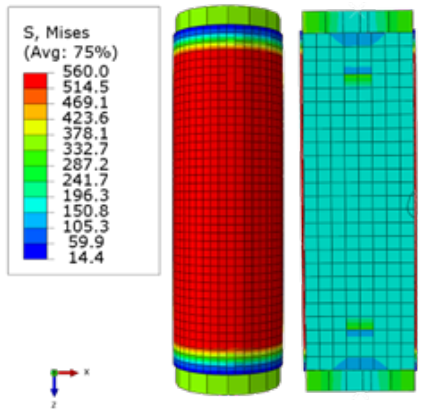

(b) C-CFC-560-110

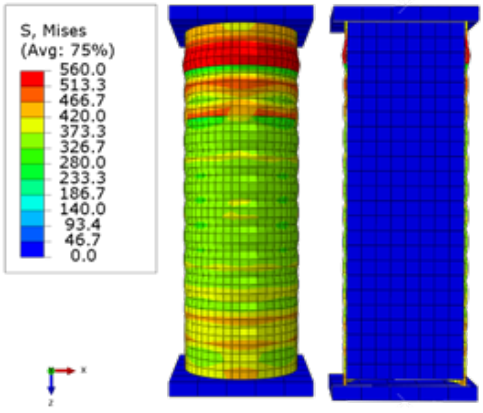

(c) C-CFS-560-110

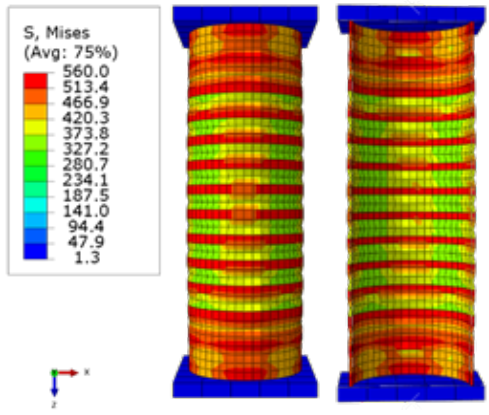

(d) C-EST-560

Figure 10. Failure modes of the columns with f_y = 560, f'_c = 110 (MPa)

For the CFS loading case, the deformation and stress distribution on the steel tube are asymmetrical across the cross-section in the middle of the column and the concrete core does not participate in the compressive load. In which, the steel tube is damaged due to reaching yield strength f_y and local buckling to the outside at the position close to the top of the column which is compressively loaded by axial displacement (Figs. 9–11(c)). Finally, for the EST loading case, Figs. 9–11(d) show the deformation and stress distribution on the steel tube symmetrically across the cross-section in the center of the column failure due to reaching yield strength f_y with local buckling both outward and inward (corrugated shape).

3.5. Axial force distribution in concrete core and steel tube

Determining the distribution of compressive forces in the concrete core and the steel tube helps to better understand the simultaneous working as well as the confinement effect of the outer steel tube on the inner concrete core. This behavior depends on the way the load is applied, in particular, the effective interaction between the steel tube wall and the concrete core occurs mainly for two loading cases, CFE and CFC. For the CFS loading case, the analysis results as shown in Figs. 9(c)–11(c) show that there is no force transfer between the steel tube wall and the concrete core. Fig. 12 shows the distribution of compressive forces on the component members of two column specimens, C-CFE-525-100 and C-CFC-525-100, during compressive loading.

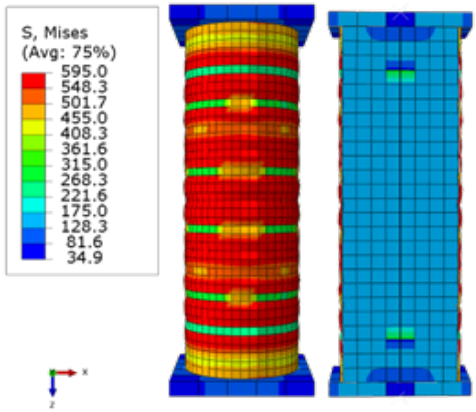

(a) C-CFE-595-120

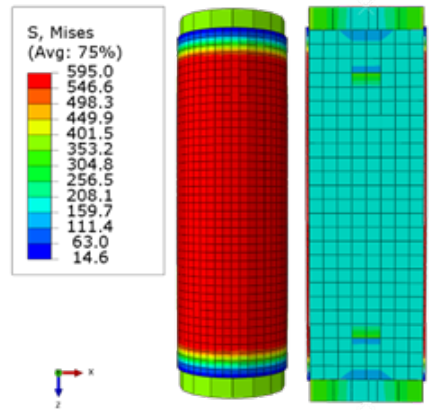

(b) C-CFC-595-120

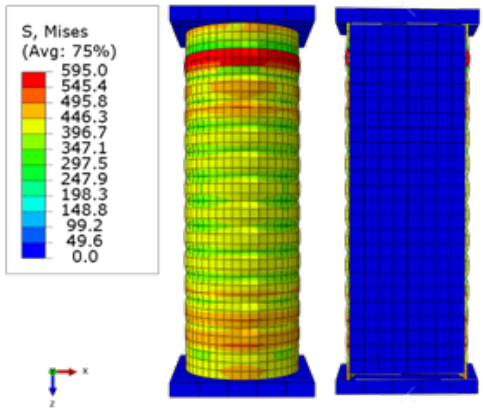

(c) C-CFS-595-120

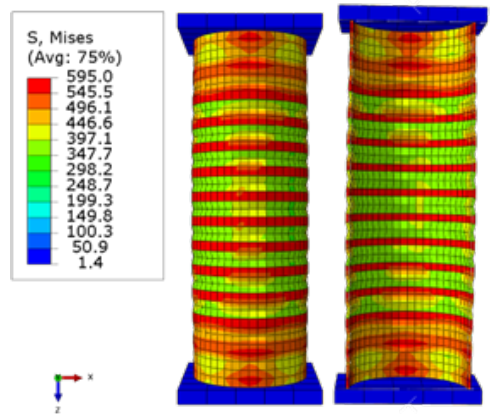

(d) C-EST-595

Figure 11. Failure modes of the columns with f_y = 595, f'_c = 120 (MPa)

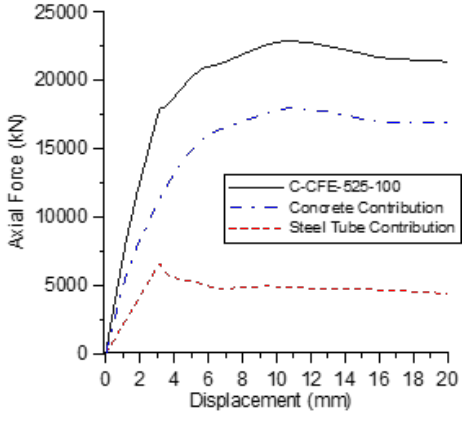

(a) Specimen C-CFE-525-100

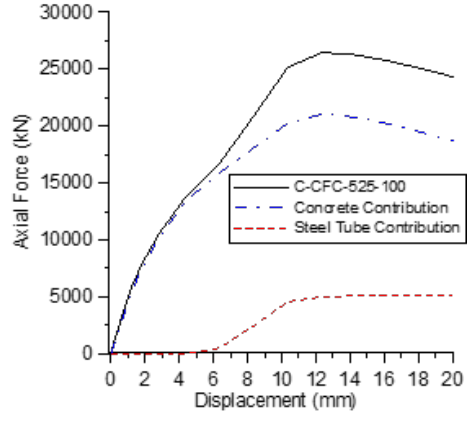

(b) Specimen C-CFC-525-100

Figure 12. Axial force distribution in CFST columns

The results in Fig. 12 show that the maximum axial compressive force in the concrete core for both CFE and CFC loading cases is larger than the compressive strength of the concrete core when

calculated according to AISC 360-16 [20]. The increase in the compressive strength of the concrete core compared to that predicted by the Standard (AISC 360-16) is due to the confinement effect of the steel tube acting on the concrete core. In which, the column specimen C-CFE-525-100 has an increase rate of 48.48% and the other one C-CFC-525-100 is 73.94%. Hence, CFST columns in the CFC loading case have the best confinement effect.

4. Conclusions

Based on the numerical simulation results in this paper, some conclusions are drawn as below:

The mechanical behavior and load-carrying capacity (compressive strength) of CFST columns depend on how the compressive load is applied to the column. In which, the CFC loading case leads to the CFST column having the highest compressive strength, increasing by 37-41% compared to the value calculated according to AISC 360-16, followed by the CFE loading case, increasing by 17-21% compared to the value calculated according to AISC 360-16, and the application of the CFS load resulted in a negligible increase in the compressive strength of the column compared to the case of loading on a hollow (empty) steel tube column, EST.

The relationship curves between axial compression force and displacement ($P - \Delta$) are similar for the same loading case when increasing the values of f_y and f_c' at various levels. In the linear elastic stage, the CFST columns with the CFE loading case have stiffer compressive behavior than that with the CFC loading case, but in the stage beyond the linear behavior then it is opposite. The other two load cases, CFS and EST, have almost identical $P - \Delta$ curves.

Increasing the values of f_y and f_c' at different levels led to a significant increase in the compressive strength of the CFST column in both CFE and CFC loading cases, but the failure mode of the column specimens in each loading case changed insignificantly. Specifically, the columns of the CFE group were damaged because the steel tube reached the yield strength and local buckling, and the concrete core could be cracked. CFST columns belonging to the CFC group were damaged due to the steel tube reaching the yield strength, and then the concrete core could be cracked. Meanwhile, columns in the CFS and EST groups were damaged because the steel tube reached yield strength and local buckling.

The confinement effect on the concrete core offerred by the steel tube leads to significantly increase the compressive strength of concrete in the two loading cases, CFC and CFE, respectively. For the CFS loading case, this effect did not occur.

Acknowledgments

The first author would like to send his thanks to The University of Danang – University of Science and Technology for the financial support to the Research project "Analysis of compressive behavior of concrete filled steel tubular columns with high strength materials", code number of Project: T2022-02-55.

References

[1] Uy, B. (1998). Concrete-filled fabricated steel box columns for multistorey buildings: behaviour and design. *Progress in Structural Engineering and Materials*, 1(2):150–158.

[2] Ge, H., Usami, T. (1992). Strength of Concrete-Filled Thin-Walled Steel Box Columns: Experiment. *Journal of Structural Engineering*, 118(11):3036–3054.

[3] Ge, H. B., Usami, T. (1994). Strength analysis of concrete-filled thin-walled steel box columns. *Journal of Constructional Steel Research*, 30(3):259–281.

[4] Schneider, S. P. (1998). Axially Loaded Concrete-Filled Steel Tubes. *Journal of Structural Engineering*, 124(10):1125–1138.

[5] Shams, M., Saadeghvaziri, M. (1999). Nonlinear Response of Concrete-Filled Steel Tubular Columns under Axial Loading. *ACI Structural Journal*, 96(6):1009–1017.

[6] Susantha, K. A. S., Ge, H., Usami, T. (2001). Uniaxial stress–strain relationship of concrete confined by various shaped steel tubes. *Engineering Structures*, 23(10):1331–1347.
[7] Hu, H.-T., Huang, C.-S., Wu, M.-H., Wu, Y.-M. (2003). Nonlinear Analysis of Axially Loaded Concrete-Filled Tube Columns with Confinement Effect. *Journal of Structural Engineering*, 129(10):1322–1329.
[8] Johansson, M., Gylltoft, K. (2002). Mechanical Behavior of Circular Steel–Concrete Composite Stub Columns. *Journal of Structural Engineering*, 128(8):1073–1081.
[9] Fujimoto, T., Mukai, A., Nishiyama, I., Sakino, K. (2004). Behavior of Eccentrically Loaded Concrete-Filled Steel Tubular Columns. *Journal of Structural Engineering*, 130(2):203–212.
[10] Han, L.-H. (2004). Flexural behaviour of concrete-filled steel tubes. *Journal of Constructional Steel Research*, 60(2):313–337.
[11] Yu, Z.-W., Ding, F.-X., Cai, C. S. (2007). Experimental behavior of circular concrete-filled steel tube stub columns. *Journal of Constructional Steel Research*, 63(2):165–174.
[12] Han, L.-H., Liu, W., Yang, Y.-F. (2008). Behaviour of concrete-filled steel tubular stub columns subjected to axially local compression. *Journal of Constructional Steel Research*, 64(4):377–387.
[13] Liu, J., Zhou, X. (2010). Behavior and strength of tubed RC stub columns under axial compression. *Journal of Constructional Steel Research*, 66(1):28–36.
[14] Yu, Q., Tao, Z., Liu, W., Chen, Z.-B. (2010). Analysis and calculations of steel tube confined concrete (STCC) stub columns. *Journal of Constructional Steel Research*, 66(1):53–64.
[15] Phan, H. D., Trinh, H. H. (2019). Analysis of mechanical behaviour of circular concrete filled steel tube columns using high strength concrete. In *Mechanics of Structures and Materials XXIV*, CRC Press, 260–265.
[16] Phan, H. D. (2021). Numerical analysis of seismic behavior of square concrete filled steel tubular columns. *Journal of Science and Technology in Civil Engineering (STCE) - HUCE*, 15(2):127–140.
[17] Son, T., Ngo-Huu, C., Thuat, D. V. (2021). Finite element modelling of rectangular concrete-filled steel tube stub columns incorporating high strength and ultra-high strength materials under concentric axial compression. *Journal of Science and Technology in Civil Engineering (STCE) - HUCE*, 15(4):74–87.
[18] Tao, Z., Wang, Z.-B., Yu, Q. (2013). Finite element modelling of concrete-filled steel stub columns under axial compression. *Journal of Constructional Steel Research*, 89:121–131.
[19] Thai, H.-T., Uy, B., Khan, M., Tao, Z., Mashiri, F. (2014). Numerical modelling of concrete-filled steel box columns incorporating high strength materials. *Journal of Constructional Steel Research*, 102:256–265.
[20] AISC 360-16. *Specification for Structural Steel Building*. Chicago, Illinois, USA.
[21] EN 1994-1-1:2004. *Eurocode 4: Design of composite steel and concrete structures - Part 1-1: General rules and rules for buildings*. European Committee for Standardization, Brussels, Belgium.
[22] AS/NZS 2327:2017. *Composite structures - Composite steel-concrete construction in buildings*. Standards Australia/Standards New Zealand, Sydney/Wellington, Australia/New Zealand.
[23] SIMULIA (2016). *Abaqus Analysis User's and Abaqus/CAE User's Guides*.
[24] Tasdemir, M. A., Tasdemir, C., Akyüz, S., Jefferson, A. D., Lydon, F. D., Barr, B. I. G. (1998). Evaluation of strains at peak stresses in concrete: A three-phase composite model approach. *Cement and Concrete Composites*, 20(4):301–318.
[25] Binici, B. (2005). An analytical model for stress–strain behavior of confined concrete. *Engineering Structures*, 27(7):1040–1051.
[26] Xiao, Q. G., Teng, J. G., Yu, T. (2010). Behavior and Modeling of Confined High-Strength Concrete. *Journal of Composites for Construction*, 14(3):249–259.
[27] Samani, A. K., Attard, M. M. (2012). A stress–strain model for uniaxial and confined concrete under compression. *Engineering Structures*, 41:335–349.
[28] Tao, Z., Wang, Z.-B., Yu, Q. (2013). Finite element modelling of concrete-filled steel stub columns under axial compression. *Journal of Constructional Steel Research*, 89:121–131.
[29] ACI 318-19. *Building Code Requirements for Structural Concrete*. Farmington Hills, Michigan, USA.